

Optical, structural, and electrical properties of Mg_2NiH_4 thin films *in situ* grown by activated reactive evaporation

R. J. Westerwaal,^{a)} M. Slaman, C. P. Broedersz, D. M. Borsa, B. Dam, and R. Griessen
Faculty of Sciences, Department of Physics and Astronomy, Condensed Matter Physics, Vrije Universiteit, De Boelelaan 1081, 1081 HV Amsterdam, The Netherlands

A. Borgschulte
GKSS-Research Center Geesthacht GmbH, WTP, Building 59 Max-Planck-Strasse 1, 21502 Geesthacht, Germany

W. Lohstroh
Institut für Nanotechnologie, Forschungszentrum Karlsruhe GmbH, Postfach 36 40 76021 Karlsruhe, Germany

B. Kooi and G. ten Brink
Department of Applied Physics, University of Groningen, Nijenborgh 4, 9747 AG Groningen, The Netherlands

K. G. Tschersich and H. P. Fleischhauer
Institut für Schichten und Grenzflächen, Forschungszentrum Jülich GmbH, 52425 Jülich, Germany

(Received 20 March 2006; accepted 25 May 2006; published online 26 September 2006)

Mg_2NiH_4 thin films have been prepared by activated reactive evaporation in a molecular beam epitaxy system equipped with an atomic hydrogen source. The optical reflection spectra and the resistivity of the films are measured *in situ* during deposition. *In situ* grown Mg_2NiH_4 appears to be stable in vacuum due to the fact that the dehydrogenation of the Mg_2NiH_4 phase is kinetically blocked. Hydrogen desorption only takes place when a Pd cap layer is added. The optical band gap of the *in situ* deposited Mg_2NiH_4 hydride, 1.75 eV, is in good agreement with that of Mg_2NiH_4 which has been formed *ex situ* by hydrogenation of metallic Pd capped Mg_2Ni films. The microstructure of these *in situ* grown films is characterized by a homogeneous layer with very small grain sizes. This microstructure suppresses the preferred hydride nucleation at the film/substrate interface which was found in as-grown Mg_2Ni thin films that are hydrogenated after deposition.

© 2006 American Institute of Physics. [DOI: [10.1063/1.2349473](https://doi.org/10.1063/1.2349473)]

I. INTRODUCTION

In recent years the complex metal hydrides Mg_2MH_x ($M=\text{Ni, Co, Fe, etc.}$) gained attention due to their potential as hydrogen storage materials and the fascinating change in optical properties upon hydrogenation. Upon hydrogen absorption Mg_2Ni transforms into Mg_2NiH_4 and contains up to 3.6 wt % of hydrogen. Mg_2MH_x thin films also show reversible optical switching at RT between a shiny metallic and a transparent semiconducting state.^{1,2} Between these two states we discovered a third optical state. This state is characterized by a low reflection (<25%) over the whole visible spectrum when measured from the substrate side, while the transmission (<0.01%) is negligible. This state is called the optical black state, since the optical absorption is at least 75%. As one can tune the hydrogen concentration and thus can switch between a reflective metal, an absorbing black and a transparent semiconducting state, these thin films are very attractive for smart coating applications,³ or hydrogen sensors.⁴

The optical black state originates from the fact that the Mg_2NiH_4 nucleates at the substrate interface upon hydrogen absorption.^{5,6} As we have shown, this results from the pecu-

liar double layer microstructure of these Mg–Ni thin films.⁷ This led us to the idea of changing the thin film microstructure by growing the film *in situ* in the hydride phase. In all previous studies the hydride phase is formed by *ex situ* hydrogenation using Pd as a catalytic cap layer. Here, we present a method to prepare complex metal hydride thin films *in situ* using activated reactive evaporation. Schoenes *et al.* reported on the optical properties of single-crystalline YH_x thin films prepared by molecular beam epitaxy in the presence of atomic hydrogen.⁸ Hayoz *et al.* also report the *in situ* growth of Y dihydride by Y evaporation under a H_2 partial pressure of 5×10^{-4} Pa.⁹ So far, the activated reactive evaporation technique has not been applied for the formation of complex metal hydride systems. We demonstrate that it is possible to deposit Mg_2NiH_4 from the atomic constituents using an atomic hydrogen source, a Knudsen source for Mg, and an electron gun for Ni. The reliable growth of semiconducting Mg_2NiH_4 requires *in situ* monitoring of the growth process. For this, we measure the optical properties and the resistivity during deposition. We find that the use of an atomic hydrogen source is essential to grow a complex hydride. During the deposition, the hydrogen pressure in the deposition chamber rises to about 2×10^{-2} Pa. This pressure is far below the equilibrium molecular hydrogen pressure of Mg_2NiH_4 . The stability of the hydride phase both in vacuum

^{a)}Electronic mail: rj.westerwaal@few.vu.nl

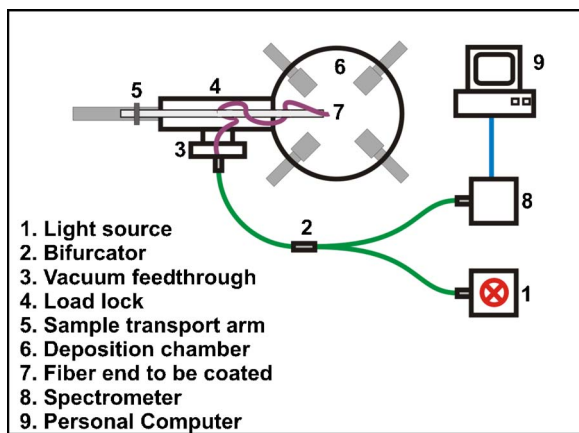


FIG. 1. (Color online) Schematic representation of the thin film deposition chamber together with the fiber setup to measure *in situ* the reflection. The film is deposited onto the freshly cleaved fiber surface.

and in air is remarkable. It shows that the dehydrogenation process has a high activation barrier.

The *in situ* growth technique opens the way for controlled doping and for constructing multilayered films of different hydride phases during deposition. In addition, it is a tool to change the thin film microstructure. Indeed, we find that the *in situ* grown films display a totally different microstructure. The self-organized bilayer segregation and the associated optically black state are absent. Both the engineering of the microstructure and the possibility of *in situ* doping are interesting from a hydrogen storage perspective.

II. DEPOSITION OF Mg_2NiH_4 THIN FILMS

Mg_2Ni thin films are prepared by coevaporation of Mg from a Knudsen cell (purity 99.98%) and Ni by means of an electron gun (purity 99.98%) in an UHV system (base pressure $<10^{-8}$ Pa). The deposition rate during evaporation is monitored using two separate quartz-crystal monitors. During deposition the resistivity of the film is continuously monitored in a four point van der Pauw geometry.¹⁰ For *ex situ* experiments the samples can be protected from oxidation by a thermally evaporated Pd cap layer (purity 99.98%). This layer catalyzes the hydrogen absorption and desorption. The chemical composition and the thickness of the as-deposited films is determined by Rutherford backscattering spectrometry (RBS). Atomic force microscopy (AFM) measurements of the surface morphology are performed *ex situ* with a Digital Instruments Nanoscope III AFM. The *ex situ* optical reflection and transmission spectra are obtained using a Bruker Fourier transform infrared (FTIR) spectrometer IFS 66/S equipped with a reflection and transmission unit.

Instead of the resistivity we can also measure *in situ* the reflection spectra during deposition, using a high temperature (HT) fiber (see Fig. 1). These types of fibers have a low degassing of the fiber jacket. Core and cladding diameter of the fiber are 200 and 230 μm , respectively. The fiber end is cleaved by using a Vytran LDC-200 autocleaver. Cleaving the fiber results in a flat and clean substrate surface. The probe fiber is clamped in a holder so that it is in line of sight

with the various sources. The other end of the fiber is glued with an UHV epoxy in a fiber-optic SubMiniature version (SMA) connector that is mounted in a feedthrough of the load lock. A bifurcator in combination with a splice bushing is used to guide the light from a tungsten-halogen source to the end of the fiber (see Fig. 1). Reflected light is guided via the second path of the bifurcator to an Ocean Optics USB 2000 charge coupled device (CCD) spectrometer. This spectrometer covers the range from 1.2 to 3.1 eV and records periodically the spectra of the reflected light during the deposition from the end of the fiber. The spectra are normalized to the corresponding calculated thin film spectrum. This technique is tested for several metallic thin films and results in a good agreement between the calculated spectrum and the *in situ* measured spectrum.

The reflection and transmission spectra of the complete optical system (fiber, fiber-film interface, film, film-vacuum interface, etc.) is calculated using a transfer matrix method that considers the Fresnel reflectance and transmittance coefficients at each interface and the absorption in each material.^{11,12} For this calculation the values of n and k of the involved materials are taken from Palik's book of optical constants.¹³

The optimization of the deposition conditions during *in situ* growth of Mg_2NiH_4 and tuning of the atomic hydrogen source will be discussed in the next section.

III. ACTIVATED REACTIVE EVAPORATION (ARE) OF Mg_2NiH_4 THIN FILMS

When growing a Mg_2NiH_4 complex metal hydride from the constituents Mg, Ni, and H atoms, the rates are tuned in such a way that the particle arrival rates at the substrate surface are optimal for hydride formation. For Mg a deposition rate of 9.9×10^{13} at./ cm^2 s and for the Ni atoms a rate of 4.6×10^{13} at./ cm^2 s is used. The partial pressure of contaminating elements, e.g., H_2O , O_2 , and CH_4 , is below 10^{-8} Pa and no contamination of the thin films is expected, which is confirmed by RBS measurements.

Hydrogen atoms are provided by a source comprising a hot capillary.^{14,15} Hydrogen gas passing the hot capillary is partly dissociated and leaves the capillary with an angular distribution peaked along the capillary axis. The hydrogen atom intensity can be controlled by the gas flow rate and the heating power of the capillary which determines its temperature. Quantitative data are given in Ref. 14. In the present experiments the gas flow rate is usually held constant and results in a hydrogen pressure at the source inlet and in the deposition chamber of 2.2×10^3 and 2×10^{-2} Pa, respectively. In reactive deposition conditions, the heating power is around 130 W rising the capillary temperature to about 2100 K. The distance from the capillary orifice to the substrate is around 15 cm. From the quantitative data mentioned above we estimate the ratio of the hydrogen to metal atom arrival rate at the substrate being around 4 which is in the order of the hydrogen to metal ratio in the Mg_2NiH_4 film (1.3). Accordingly, every third impinging atom is incorporated into the growing film.

We measure the resistivity during deposition to deter-

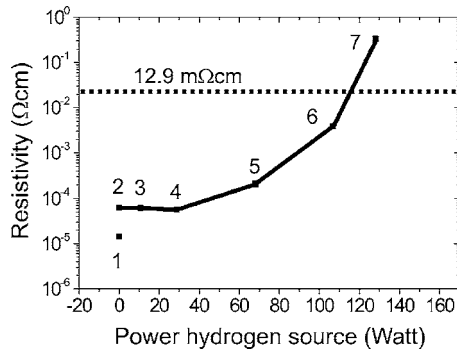


FIG. 2. *In situ* resistivity measurement for activated reactive evaporation of Mg_2NiH_x thin films. Each point in the figure represents another 200-nm-thick Mg_2NiH_x film deposited at the corresponding capillary power (see text). The horizontal line at 12.9 m Ω cm indicates the resistivity of an *ex situ* hydrogenated film. Point 1: resistivity of a metallic Mg_2Ni thin film deposited at 5×10^{-7} Pa. Points 2–7: resistivity at an increasing heating power of the atomic hydrogen source capillary. The resistivity increases from 1.45×10^{-5} to 0.34Ω cm.

mine the dependence of the hydride growth on the flux of atomic hydrogen provided by the hydrogen source. Given the five orders of magnitude higher resistivity of the hydride phase, the change in electrical properties is a good indication for the amount of hydride formed.¹⁶

We plot the film resistivity versus heating power of the H source capillary (see Fig. 2). Each point in the figure represents a fresh 200-nm-thick Mg_2NiH_x film deposited at the corresponding capillary power. Point 1 indicates the resistivity of a metallic Mg_2Ni film prepared at a background pressure of 2×10^{-7} Pa (vacuum conditions). Under these conditions, films with a resistivity of $\rho = 1.45 \times 10^{-5} \Omega$ cm are obtained. This measured resistivity is usually found in metallic Mg_2Ni films.^{5,6,16} Using hydrogen, i.e., supplying molecular hydrogen at a pressure of 2×10^{-2} Pa through the source without heating the capillary, results in a slightly higher resistivity (point 2 in Fig. 2). This means that the film contains only a very small amount of hydrogen. Obviously the growth of the hydride phase is impossible simply by using molecular hydrogen since we operate below the hydrogen equilibrium pressure of 50 Pa. Keeping the gas flow rate constant and increasing the amount of atomic hydrogen by increasing the heating power to 128 W (2100 K), we observe an increase of the resistivity to 0.34Ω cm (point 7 in Fig. 2). The resistivity of the exposing film increases almost by five orders of magnitude indicating the formation of a semiconducting phase, Mg_2NiH_4 or MgH_2 . As we will show optically, we can identify the film as Mg_2NiH_4 . Reducing the deposition rate of the Mg and Ni atoms, to obtain a larger H/M ratio, does not result in a higher resistivity value. Once a 200 nm hydride thin film is grown; the deposition of Mg and Ni as well as the gas flow through the source is terminated; the deposition chamber is pumped down to 2×10^{-7} Pa. Remarkably, the resistivity does not change. Apparently, the hydride is stable and does not lose hydrogen although the pressure is much below the hydrogen equilibrium pressure of Mg_2NiH_4 . This means that the dehydrogenation reaction is kinetically blocked.

Enache *et al.* reported a detailed investigation of the electronic transport properties of Mg_2NiH_x thin films

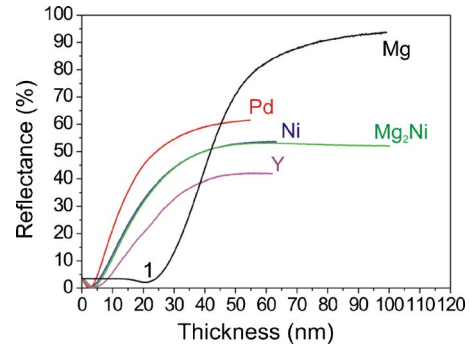


FIG. 3. (Color online) Reflectance of Ni, Pd, Mg, Y, and Mg_2Ni films at an energy of 1.95 eV as a function of thickness as measured by a QCM. The beginning of the spectra is characterized by a minimum in reflectance for all the measured elements at a certain thickness. Above a certain thickness the reflectance reaches a constant value and the films become optically closed.

(capped with a discontinuous 2 nm Pd layer).¹⁶ For *ex situ* hydrided films they found a resistivity of 12.9 m Ω cm and concluded that Mg_2NiH_4 behaves as a heavily doped semiconductor. This resistivity value is an order of magnitude lower than for our *in situ* grown Mg_2NiH_4 thin films. As we will see later, the grain boundary density of these *in situ* grown films is much higher than those prepared by *ex situ* hydrogenation of Mg_2Ni films. This observation may explain the difference between the resistivity value found by Enache *et al.* and our *in situ* grown films.

In the next sections the optical characterization of the films both during and after deposition substantiates our claim that we indeed form Mg_2NiH_4 . Before we describe our results on *in situ* grown Mg_2NiH_4 thin films, we briefly discuss the optical reflection spectra obtained during deposition of elemental metallic thin films.

IV. FIBER SPECTROSCOPY OF THIN METAL FILMS

The reflection at an energy of 1.95 eV as a function of the film thickness [measured with a quartz-crystal monitor (QCM)] is shown for Ni, Pd, Mg, Y, and Mg_2Ni in Fig. 3. The reflection starts with a decrease in reflection within 10 nm thickness for all the elements except Mg, resulting in a temporary minimum. Upon further deposition the thin film becomes optically closed and the reflection reaches a constant value. The reason for the anomalous behavior of Mg is probably the low sticking of Mg atoms on a bare substrate/fiber compared to the measured thickness by the QCM.⁷

Caranto *et al.* also observe this reflection minimum in their measurements but they do not give a proper explanation of the formation of the minimum in reflectance.¹⁷ Emmerson *et al.* argue that this effect can result from a change in electronic structure¹⁸ of both the growing layer and the substrate. Furthermore, a decrease in the free carrier density will also result in a decrease in reflectance.¹⁹ Butler and Buss assume that the minimum of the reflectance is typical for noble metals.^{20,21} Heavens points out that the minimum in reflectance is precisely in accordance with the theory of a thin homogeneous film and is observed for many metallic layers. Although they describe thin film optics quite extensively for several kinds of films, the origin of this effect is not explained explicitly. Furthermore, they state that the position of

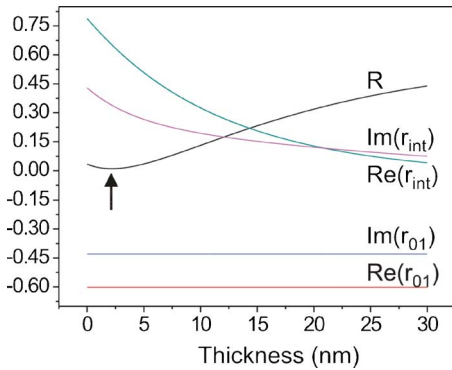


FIG. 4. (Color online) Reflectance (R) as calculated by Eq. (1). The imaginary part of r_{01} and r_{int} [$\text{Im}(r_{01}), \text{Im}(r_{\text{int}})$] and the real part of r_{01} and r_{int} [$\text{Re}(r_{01}), \text{Re}(r_{\text{int}})$] are shown. It is clear that r_{01} is constant and negative (this is due to the phase change when reflecting at an interface). R_{int} is positive and decreases monotonically (as one expects due to the higher absorption in the layer with increasing thickness). The interference of r_{01} and r_{int} is destructive for all d because the two contributions are out of phase. The destructive interference is obviously largest when $|r_{01} + r_{\text{int}}|$ has a minimum value.

the minimum is wavelength dependent for gold, silver, and iron but not for platinum and that there is a discrepancy between the theoretical calculated reflection and experiment due to the thin film microstructure, which influences the n and k values of thin films.

To establish the physical origin of this behavior, we calculate the reflectance for a single film with Eq. (1),^{11,12}

$$R(\omega) = \left| \frac{r_{01} \exp[-i\delta(d)(n_1 + ik_1)] + r_{12} \exp[i\delta(d)(n_1 + ik_1)]}{\exp[-i\delta(d)(n_1 + ik_1)] + r_{01}r_{12} \exp[i\delta(d)(n_1 + ik_1)]} \right|^2, \quad (1)$$

in which r_{ij} is the reflection at the interface ij . The film thickness enters Eq. (1) implicitly through the dimensionless parameter $\delta(d)$ that governs the phase shift and the damping of the wave upon crossing the entire film, n_i is the refractive index, and k_i the extinction coefficient. Equation (1) predicts a reflectance minimum at a thickness of 2.1 nm for a fiber/Ni/vacuum system (we find similar values for the other metals/alloys Pd, Mg₂Ni, Y, etc.). This means that the characteristic minimum we observe is a direct consequence of Eq. (1). Since this calculation does not make use of a variation of n and k as function of deposited thickness or film microstructure, this implies that the minimum is due to the thickness dependence of the reflectance described by this equation.^{11,12} Equation (1) can be rewritten as Eq. (2),

$$R(\omega) = \left| r_{01} + \frac{r_{12}(1 - r_{01}^2) \exp[2i\delta(d)(n_1 + ik_1)]}{1 + r_{01}r_{12} \exp[2i\delta(d)(n_1 + ik_1)]} \right|^2. \quad (2)$$

There are two terms: r_{01} is the reflectance from the fiber/film interface and the second term, in this paper indicated as r_{int} , is the contribution from multiple internal reflections inside the growing film. In Fig. 4 the magnitude of the real and imaginary part of r_{01} and r_{int} are plotted versus film thickness. The real and imaginary part of r_{01} ($\text{Re } r_{01}$ and $\text{Im } r_{01}$, respectively) are constant and negative (which is due to the phase change accompanying the reflection at the fiber-film

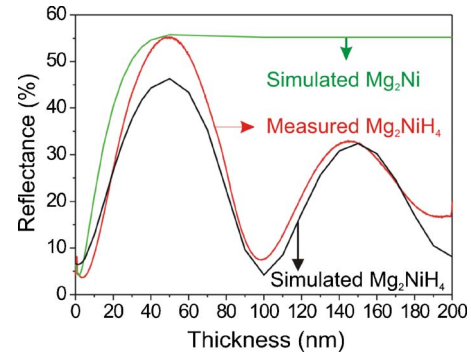


FIG. 5. (Color online) Reflectance at 1.95 eV vs deposited Mg₂NiH₄ thickness (red curve). The simulated reflectance of a Mg₂Ni thin film (black curve) and of a Mg₂Ni thin film (green curve) are also shown. The good agreement between the measured reflectance and simulated reflectance indicates that Mg₂NiH₄ is synthesized *in situ*.

interface). The real part and imaginary part of r_{int} ($\text{Re } r_{\text{int}}$ and $\text{Im } r_{\text{int}}$, respectively) are positive and decrease monotonically. This is what one expects for the absorption of a layer which increases in thickness. The interference of r_{01} and r_{int} is destructive for all d because the two contributions are out of phase. As the contribution of r_{int} is larger than that of r_{01} for thicknesses < 2.1 nm, the sum of r_{01} and r_{int} is positive. Since r_{int} is decreasing as function of thickness, the destructive interference is obviously largest when $|r_{01} + r_{\text{int}}|$ is minimal (R is minimal and in this case at $d=2.1$ nm, as indicated by the arrow). As r_{int} dies out, the sum of r_{01} and r_{int} becomes more negative. However, due to the fact that R is defined as $R=|r_{01} + r_{\text{int}}|^2$, R becomes more and more positive as r_{int} dies out. This means that the dip in reflection originates from the destructive interference due to the phase change upon reflection from the surface of the growing layer combined with an increase of absorption due to the growing film thickness.

Our calculations show that we can explain the minimum in reflection by a complete theoretical description without assuming changes in n and k values as function of thickness or microstructure. Therefore the result is true for all materials and the position of the minimum is wavelength sensitive (depends on n and k).

V. IDENTIFICATION OF *IN SITU* GROWN Mg₂NiH₄

The phase of the growing film can be identified via *in situ* measurement of the reflection. Figure 5 shows the reflectance versus thickness of an as-grown Mg₂Ni and a Mg₂NiH₄ as well as the numerical simulation of a Mg₂NiH₄ film at 1.95 eV. The reflectance measured during activated reactive evaporation exhibits a well defined interference pattern. This pattern arises from the reflections of the fiber/film and film/vacuum interfaces and indicates the growth of a transparent film. Apart from a small overshoot at the interference maximum and minimum, the measured reflection spectrum is identical to the calculated spectrum for a homogeneous Mg₂NiH₄ thin film. This indicates that we indeed grow a Mg₂NiH₄ hydride phase from the individual elements Mg, Ni, and H. The reflectance measured *in situ* as function of energy and the corresponding calculated reflectance spec-

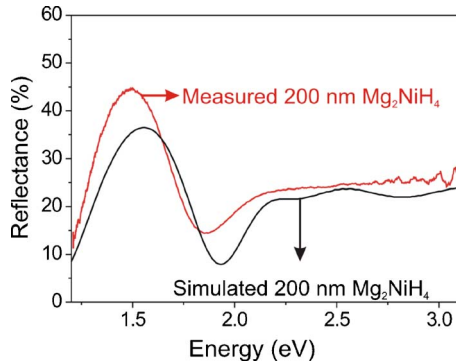


FIG. 6. (Color online) Reflection spectrum vs energy for a 200 nm Mg_2NiH_2 thin film (red curve). The simulated spectrum of Mg_2NiH_4 (black curve) indicates that we indeed grow the hydride phase. It is shifted by 0.15 eV as compared with the measured spectrum.

trum are shown in Fig. 6. Except for a small redshift in energy of 0.15 eV, the measured and calculated spectra are very similar in shape.

The reflection and transmission spectra of the *in situ* grown Mg_2NiH_4 hydride film were also measured *ex situ* using a Bruker spectrometer (see Figs. 7 and 8). It is remarkable that the film remains stable when it is taken out of the vacuum system. The resistivity and optical measurements do not change when exposing the *in situ* grown film to air/oxygen. From experiments we know that if we bring this film in contact with air there is still no dehydrogenation. Even after depositing subsequently a Pd cap layer on the film, the film does not unload anymore up to temperatures of 373 K (films capped with Pd directly after deposition can be loaded-unloaded at RT). This shows that on exposure to air/oxygen a passivated surface layer forms on top of the hydride, which is limited in thickness (no optical effect is observed) and blocks the desorption of hydrogen. Probably an oxide skin develops on top of the film which prevents dehydrogenation, but we could not yet identify its nature. The *ex situ* measured reflection spectrum is very similar to the calculated spectrum (see Fig. 7) with the same small redshift of 0.15 eV. The transmission spectrum shows a band gap of 1.75 eV (see Fig. 8). This is close to the band gap of an *ex situ* hydrogenated Mg_2Ni thin film, 1.9 eV,^{5,6} which con-

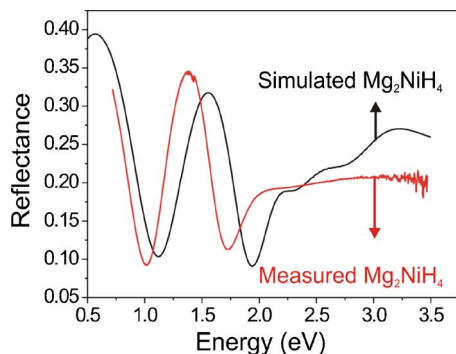


FIG. 7. (Color online) *Ex situ* measured reflection spectrum for an *in situ* grown 200 nm Mg_2NiH_4 thin film without a Pd cap layer (red curve). The spectrum displays a 0.15 eV redshift which is also observed in the *in situ* measured spectrum. The interference pattern of the simulated reflectance is comparable to the interference pattern of the measured reflectance.

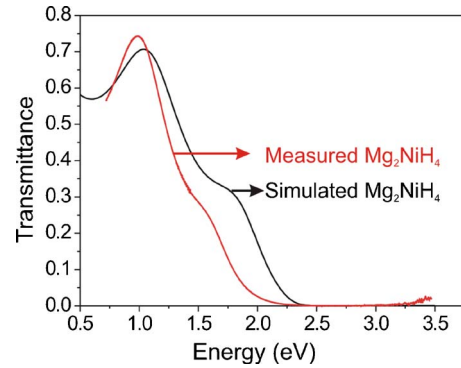


FIG. 8. (Color online) *Ex situ* measured transmission spectrum for an *in situ* grown 200 nm Mg_2NiH_4 thin film without a Pd cap layer (red curve). We observe that the measured transmittance has an optical band gap of 1.75 eV and the simulated transmittance has an optical band gap of 1.9 eV.

firms the direct formation of Mg_2NiH_4 by activated reactive evaporation. If we would have formed the only other possible hydride phase, MgH_2 , we would observe a shift of the band gap towards much higher energies, because the band gap of MgH_2 is 5.6 eV.²²

The redshift in the apparent optical band gap might be due to a higher purity of the *in situ* grown film. As the apparent gap in heavily doped semiconductors decreases with the dopant level, the lower dopant level of our *in situ* films might explain the observed reduction.²³ The shift of E_g is given by the Burstein-Moss equation,

$$\Delta E_g = \frac{\hbar^2}{2m_{\text{ch}}^*} (3\pi^2 N_{\text{opt}})^{2/3}, \quad (3)$$

in which m_{ch}^* is the reduced effective mass, and N_{opt} the optical carrier concentration. The 0.15 eV band gap shift results in $2.64 \times 10^{20}/\text{cm}^3$ charge carriers, which is one order of magnitude lower than found by Enache *et al.*¹⁶ for *ex situ* hydrided Mg_2Ni thin films. This nicely resembles the difference in resistivity which is one order of magnitude higher in our *in situ* grown films as compared to the *ex situ* hydrided films.

VI. THE OPTICAL SWITCHING OF Mg_2NiH_4 THIN FILMS

Before describing the optical behavior of the *in situ* grown films, we shortly summarize that of an *ex situ* hydrided Mg_2NiH_4 film.

When a Mg_2Ni film is exposed to hydrogen the reflection drops to a minimum value at which the transmission is still essentially zero (see Fig. 9). Transmission starts to increase after the reflection has recovered from its minimum value. This results in an intermediate optically black state and is a consequence of the self-organized double layering of these films upon hydrogenation. This double layering has its origin in a preferred hydride nucleation at the film/substrate interface. Lohstroh *et al.* have shown that it is not possible to find a single set of n and k that describes the observed R and T spectra during the optical black state (maximal absorption) and that one needs to assume a double layer model.^{5,6}

To examine the rehydrating properties of an *in situ* grown Mg_2NiH_4 film, we cap the film *in situ* with 10 nm Pd.

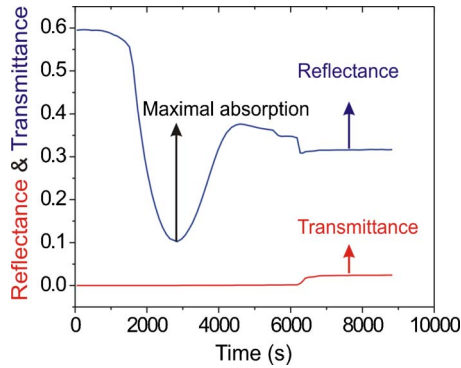


FIG. 9. (Color online) Reflection and transmission spectra at 1.25 eV vs hydrogenation time of an as-prepared Mg_2Ni thin film. At the minimum of the reflectance (blue curve), the transmittance (red curve) is essentially zero, indicating the preferred hydride nucleation at the interface with its maximal absorption.

This results in the dehydrogenation of the hydride phase and enables us to rehydrogenate the film. The rehydrogenation of the *in situ* grown Mg_2NiH_4 thin films displays a clear difference in hydrogenation behavior (see Fig. 10). The minimum in reflection is less pronounced and before the reflection reaches its minimum value, the transmission has already increased to $T=0.035$. This means that the hydride nucleates throughout the entire film and not solely at the film/substrate interface. Thus we can find an “effective” n and k for this film. Therefore we make a calculation of the reflectance and transmittance by the transfer matrix method as described previously. This method calculates R and T spectra for a dense grid of (n, k) for the Mg_2NiH_x layer. A crossing of R and T indicates a solution (n, k) . For $R=0.1$ and $T=0.035$ we find two sets of effective (n, k) (see Fig. 11). This implies that the film behaves as a homogeneous layer, and can be described by an effective medium theory. Furthermore, this indicates that there is almost no preferred hydride nucleation at the substrate interface. In the next section we will show that this is related to the thin film microstructure, which is quite different from that of films that are grown without a hydrogen background pressure.

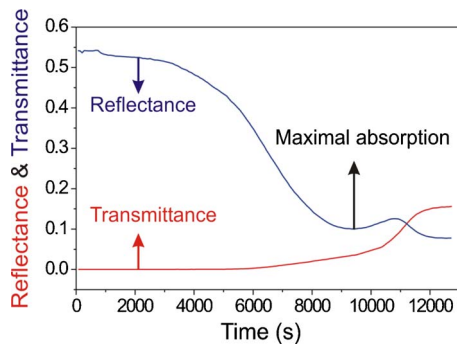


FIG. 10. (Color online) Reflection and transmission spectra at 1.25 eV vs hydrogenation time of a film which was *in situ* deposited as Mg_2NiH_4 and then dehydrogenated. At the reflectance minimum (blue curve), the transmittance (red curve) has a finite value of 0.04. This finite value of the transmittance indicates that we can model the Mg_2NiH_x layer by a single set of n and k values during the maximal absorption.

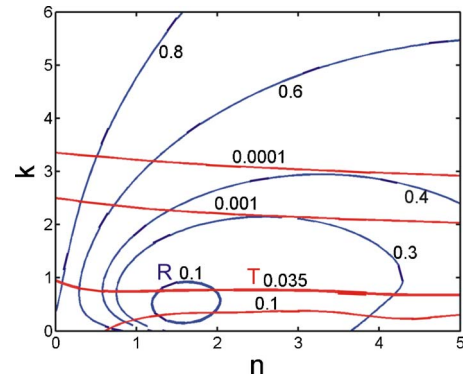


FIG. 11. (Color online) Contour maps of the reflectance and transmittance at 1.25 eV for a 200 nm Mg_2NiH_x thin film capped with 10 nm Pd on quartz. The crossing of the contour plot for transmittance at $T=0.035$ and the reflectance at $R=0.1$ (which correspond to the values for a film in the black state) indicates that optically the Mg_2NiH_x film can be modeled as a homogeneous layer.

VII. MICROSTRUCTURE OF *IN SITU* GROWN Mg_2NiH_4 THIN FILM

The surface morphology of the *in situ* prepared Mg_2NiH_4 thin films is investigated by AFM measurements. A comparison between an as-prepared Mg_2Ni , an *ex situ* postdeposition hydrided Mg_2NiH_4 film, and an *in situ* grown Mg_2NiH_4 film is shown in Fig. 12. The grains of a 200 nm *ex situ* hydrided Mg_2NiH_4 film have an average size of 75 nm in diameter [see Fig. 12(b)] which is comparable to an unloaded Mg_2Ni film [see Fig. 12(a)]. The surface microstructure of an *in situ* prepared Mg_2NiH_4 film has a significantly smaller grain size of 25 nm. Furthermore, the roughness of the unloaded Mg_2Ni film surface has decreased and is in the order of 1 nm, whereas a normal 200 nm Mg_2NiH_4 film has a roughness of 20 nm [see Fig. 12(b)].

With AFM we can only probe the film surface. We use scanning electron microscopy (SEM) measurements on cleaved 200 nm *in situ* prepared Mg_2NiH_4 films deposited on Si substrates, to investigate the microstructural cross section of the film. The specific columnar microstructure of Mg_2Ni thin films with the typical small grain structure near the substrate interface has disappeared in the *in situ* prepared Mg_2NiH_4 films [see Figs. 13(a) and 13(b)]. The *in situ* grown thin film consists of a homogeneous phase without any noticeable microstructure and the film microstructure is smaller than or close to the resolution of the SEM apparatus (maximum resolution of 1.5–2.0 nm). Preliminary plane view transmission electron microscopy (TEM) measurements show that these films are close to an amorphous phase and

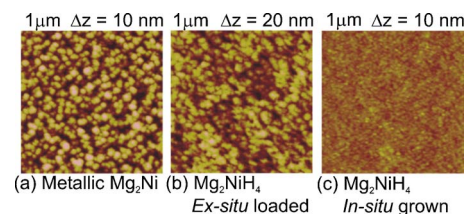


FIG. 12. (Color online) AFM measurements on (a) a 200 nm Mg_2NiH_4 thin film covered by 10 nm of Pd and (b) a 200 nm $\text{Mg}_2\text{NiH}_{4-\delta}$ thin film prepared by activated reactive deposition.

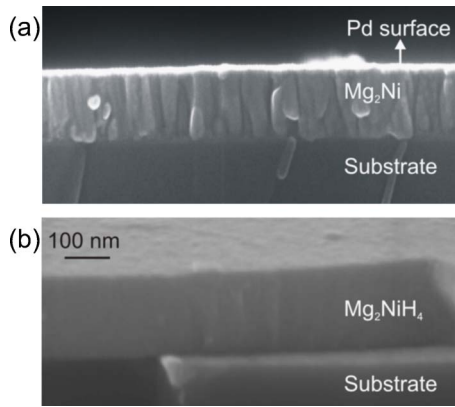


FIG. 13. (Color online) (a) SEM image of the cross section of an as-deposited 200 nm Mg_2Ni . The film shows a clear columnar structure. (b) SEM cross-sectional image of a 200 nm Mg_2NiH_4 thin film prepared by activated reactive deposition. The surface of the film is very flat as compared to the Mg_2Ni film.

that the crystallites are probably around 1 nm. These measurements imply that there is no microstructural reason for a preferred hydride nucleation as is the case for an *ex situ* hydrided Mg_2NiH_x thin film. This is consistent with the optical measurements in Sec. VI where we concluded that the hydride nucleates throughout the whole thin film, and not just at the substrate interface.

VIII. THE STABILITY OF Mg_2NiH_4 AND THE ROLE OF PD

The atomic hydrogen source allows us to grow *in situ* Mg_2NiH_4 thin films at an applied hydrogen pressure below the H_2 equilibrium pressure of Mg_2NiH_4 formation. Schoenes *et al.* found that they could grow $\text{YH}_{2.1}$ hydride films at an ambient hydrogen gas pressure of 1.3×10^{-4} Pa, whereas the equilibrium pressure of the films to form $\text{YH}_{2.1}$ is lower.⁸ Hayoz *et al.* also reports about the *in situ* growth of Y dihydrides⁹ by applying a hydrogen gas pressure. While the atomic hydrogen source is essential for the hydride formation in complex hydride systems, the blocked decomposition reaction stabilizes the hydride formed. Indeed, the *in situ*

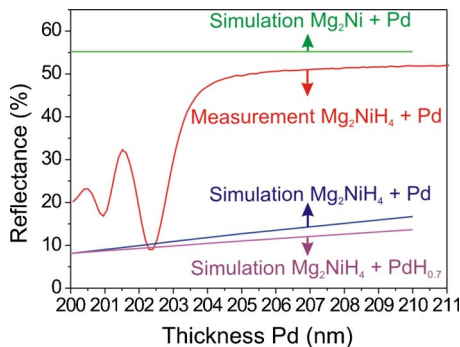


FIG. 14. (Color online) Reflectance at 1.95 eV as a function of deposited Pd thickness on an *in situ* grown 200 nm Mg_2NiH_4 hydride film. Simulation of the reflectance of a 200 nm Mg_2NiH_4 film capped with Pd and capped with $\text{PdH}_{0.7}$ are shown together with a 200 nm metallic $\text{Mg}_2\text{Ni}/\text{Pd}$ film. The developing interference pattern indicates the unloading of the film with the metallic Mg_2Ni phase forming from the Pd surface downwards. The simulations with Pd and $\text{PdH}_{0.7}$ indicates that the film really unloads and that the change in reflectance is not due to the deposited Pd cap layer.

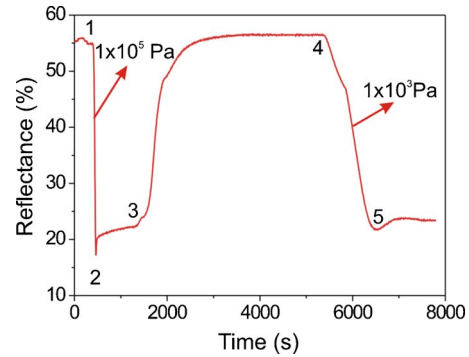


FIG. 15. (Color online) Reflection spectra at 1.95 eV during the loading/unloading process at room temperature of an *in situ* grown Mg_2NiH_4 thin film. Point 1: Start of the rehydrogenation at 1×10^5 Pa of an *in situ* prepared Mg_2NiH_4 film which was unloaded after it was capped with Pd. Point 2: Indicating the reduced minimum in reflection. Point 3: Start to unload the thin films in air. Point 4: Start of a rehydrogenation but now at 1×10^3 Pa. Point 5: Again the reduced minimum in reflection is observed.

grown Mg_2NiH_4 hydride film remains in its metastable state in vacuum (5×10^{-7} Pa) after deposition. The hydrogen desorption from the film without a Pd cap layer is almost negligible on at least a time scale of hours. This shows that the dehydrogenation process of Mg_2NiH_4 has a high activation barrier and is kinetically blocked. Depositing a Pd cap layer on top of an *in situ* grown hydride film results in a spontaneous dehydrogenation of the film. This process starts already at only a few angstrom of Pd (see Fig. 14). The deposition of a 10 nm Pd cap layer results in a completely unloaded Mg_2Ni metallic film within minutes, under high vacuum (HV) conditions. After rehydrogenating this film in the vacuum system (load lock), the unloading kinetics have become much slower than before. However, when we subject the film to air, the hydrogen desorption is accelerated and the film unloads to the metallic phase within minutes; see point 3 in Fig. 15 and point 4 in Fig. 16. The need to activate the dehydrogenation by O_2 is always observed in *ex situ* hydrided Pd/ Mg_2NiH_4 thin films. It seems as if the hydrogenation of the Pd-covered metal alloy has a detrimental effect on the activation energy for dehydrogenation.

Gräsjö *et al.* performed a study on the surface reaction of

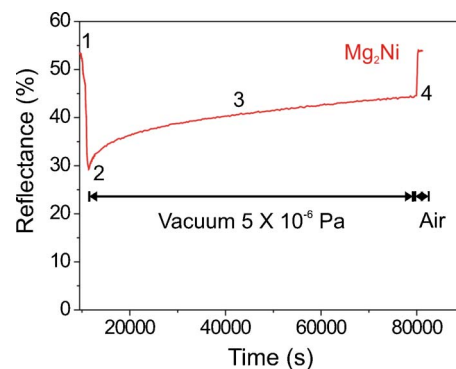


FIG. 16. (Color online) Reflectance at 1.95 eV of a postdeposition hydrogen absorption/desorption cycle of an *in situ* grown 200 nm Mg_2NiH_4 thin film capped with 10 nm Pd. Point 1: Unloaded Mg_2Ni phase. Point 2: Reduced interference minimum. Point 3: Hydrogen desorption in vacuum. Point 4: Applied atmospheric air environment. The exposure to an air environment catalyzes the dehydrogenation tremendously.

palladium hydride in vacuum, air, and water.²⁴ They found that the activation energy of desorption of hydrogen is lowered by the reaction with oxygen. Furthermore a humid atmosphere catalyzes the reaction between hydrogen and oxygen and increases the release rate of hydrogen by a factor of 100 as compared to desorption in a vacuum system. In a vacuum system the release of hydrogen can only take place by the recombination and desorption process of hydrogen. It is difficult to understand the difference between the unloading of the *in situ* grown hydride in vacuum and that of the rehydrided film, because the dehydrogenation conditions are the same in both cases.

Possibly contamination of the Pd and the intermixing of Pd with Mg₂NiH₄ play a role here. Although the applied hydrogen gas to rehydrogenate the film is 99.999 pure, contaminants which degrade the catalytical properties of the Pd. This is, however, not plausible since the same hydrogen gas is used in the *in situ* growth.

Alternatively, Borgschulte *et al.* suggests that the Pd may become covered by the hydride metal on hydrogenation. This so-called strong-metal support interaction (SMSI) effect is driven by the minimization of the surface energy and plays a large role in the reduced catalytic properties of the Pd cap layer.^{25,26}

IX. CONCLUSIONS

In situ fiber spectroscopy and *in situ* resistivity measurements show that complex metal hydride thin films can be grown by an activated reactive evaporation. Mg₂NiH₄ hydride thin films can be grown from the constituent elements Mg, Ni, and H, where H is provided by an atomic hydrogen source. The hydride films are stable in vacuum. Only when adding Pd, the as-grown hydride films transform to the metallic state. The dehydrogenation of a rehydrided film is much more difficult and requires oxygen. The difference in dehydrogenation behavior of an *in situ* grown Mg₂NiH₄ thin film and a rehydrogenated thin film may have its origin in a contamination effect of the Pd catalyst or a microstructural reorganization upon rehydriding the thin film. Further research has to be done to clarify the origin of this effect.

In situ resistivity measurements show that the resistivity of an *in situ* grown Mg₂NiH₄ thin film is 0.34 Ω cm, which is an order of magnitude higher than for a postdeposition hydrided film. This mismatch between *in situ* and *ex situ* hydrided films can be attributed to the high density of hydride grain boundaries in *in situ* prepared hydrides. The shift of the energy band gap indicates a low charge carrier density, which may also contribute to the high resistivity value.

During deposition, a minimum in reflection is observed, which is caused by a two-step process. A destructive interference due to the phase change upon reflection from the growing layer and an increasing absorption due to this increase in the film thickness. No assumptions about the thin film microstructure or thickness dependence of the *n* and *k* values need to be made to clarify this effect.

As proposed in a previous paper, here we proved the relation between the preferred hydride nucleation in Mg₂Ni thin films and the specific microstructure of these films. Thin films grown by activated reactive evaporation, consists of a small grained homogeneous layer and since there is no microstructural development throughout the film, there is no preferred hydride nucleation inside the film. Since we do not observe an optical black state in these films, we conclude that the occurrence of this effect in *ex situ* Mg₂Ni films is due to its peculiar microstructure.

ACKNOWLEDGMENTS

This work is part of the research program of the Stichting voor Fundamenteel Onderzoek der Materie (FOM), financially supported by the Nederlandse Organisatie voor Wetenschappelijk Onderzoek (NWO). The authors are grateful to H. Schreuders and J. H. Rector for technical support.

¹T. J. Richardson, J. L. Slack, R. D. Armitage, R. Kostecki, B. Farangis, and M. D. Rubin, *Appl. Phys. Lett.* **78**, 3047 (2001).

²T. J. Richardson, J. L. Slack, B. Farangis, and M. D. Rubin, *Appl. Phys. Lett.* **80**, 1349 (2002).

³J. L. M. van Mechelen, B. Noheda, W. Lohstroh, R. J. Westerwaal, J. H. Rector, B. Dam, and R. Griessen, *Appl. Phys. Lett.* **84**, 3651 (2004).

⁴M. Slaman, B. Dam, M. Pasturel, D. M. Borsa, H. Schreuders, J. H. Rector, and R. Griessen, *Sens. Actuators B* (submitted).

⁵W. Lohstroh, R. J. Westerwaal, B. Noheda, I. A. M. E. Giebels, B. Dam, and R. Griessen, *Phys. Rev. Lett.* **93**, 197404 (2004).

⁶W. Lohstroh, R. J. Westerwaal, J. L. M. van Mechelen, C. Chacon, E. Johansson, B. Dam, and R. Griessen, *Phys. Rev. B* **70**, 165411 (2004).

⁷R. J. Westerwaal, A. Borgschulte, W. Lohstroh, B. Kooi, G. ten Brink, M. J. P. Hopstaken, P. H. L. Notten, and B. Dam, *J. Alloys Compd.* **416**, 2 (2006).

⁸J. Schoenes, M. Rode, H. Schröter, D. Zur, and A. Borgschulte, *J. Alloys Compd.* **404–406**, 453 (2005).

⁹J. Hayoz, Th. Pillo, M. Bovet, A. Zuttel, St. Guthria, G. Pastore, L. Schlappbach, and P. Aebi, *J. Vac. Sci. Technol. A* **18**, 2417 (2000).

¹⁰L. J. van der Pauw, *Philips Res. Rep.* **13**, 1 (1958).

¹¹O. S. Heavens, *Optical Properties of Thin Solid Films* (Dover, New York, 1965).

¹²A. T. M. van Gogh, *Probing the Metal-Insulator Transition in Rare-Earth Based Switchable Mirrors* (Vrije Universiteit, Amsterdam, 2001).

¹³*Handbook of optical constants of solids*, edited by E. D. Palik (Academic, San Diego, 1998), Vols. I–III.

¹⁴K. G. Tschersich and V. von Bonin, *J. Appl. Phys.* **84**, 4065 (1998).

¹⁵K. G. Tschersich, *J. Appl. Phys.* **87**, 2565 (2000).

¹⁶S. Enache, W. Lohstroh, and R. Griessen, *Phys. Rev. B* **69**, 115326 (2004).

¹⁷N. R. Y. Caranto, S. C. Kaddu, J. Szajman, M. M. Murphy, S. F. Collins, and D. J. Booth, *Meas. Sci. Technol.* **4**, 865 (1993).

¹⁸C. M. Emmerson, T.-H. Shen, S. D. Evans, and H. Allinson, *Appl. Phys. Lett.* **68**, 3740 (1996).

¹⁹F. Wooten, *Optical Properties of Solids* (Academic, New York, 1972).

²⁰M. A. Butler and R. J. Buss, *Sens. Actuators B* **11**, 161 (1993).

²¹M. A. Butler, *Sens. Actuators B* **22**, 155 (1994).

²²I. A. M. E. Giebels, J. Isidorsson, and R. Griessen, *Phys. Rev. B* **69**, 205111 (2004).

²³H. Fujiwara and M. Kondo, *Phys. Rev. B* **71**, 075109 (2005).

²⁴L. Grasjö, G. Hultquist, K. L. Tan, and M. Seo, *Appl. Surf. Sci.* **59**, 135 (1992).

²⁵A. Borgschulte, R. J. Westerwaal, J. H. Rector, B. Dam, R. Griessen, and J. Schoenes, *Phys. Rev. B* **70**, 155414 (2004).

²⁶A. Borgschulte, R. Gremaud, S. de Man, R. J. Westerwaal, J. H. Rector, B. Dam, and R. Griessen, *Appl. Surf. Sci.* (in press).